Heliyon 9 (2023) e21892

Contents lists available at ScienceDirect

Heliyon

journal homepage: www.cell.com/heliyon

S14G-humanin confers cardioprotective effects against chronic adrenergic and pressure overload-induced heart failure in mice

Qi Zhao [a,1], Ming-Ming Cai [a,1], Dan Li [a], Bin-Yi Zhao [a], Shuang-Shan Zhou [a], Zhen-Ru Wu [b], Yu-Jun Shi [b], Li Su [a,*]

[a] Department of Cardiology, The Second Affiliated Hospital of Chongqing Medical University, Chongqing, 400010, China
[b] Laboratory of Pathology, West China Hospital, Sichuan University, Chengdu, Sichuan, 610041, China

ARTICLE INFO

Keywords:
S14G-humanin
Heart failure
Cardiac remodeling
TGF-β

ABSTRACT

S14G-humanin (HNG), an analog of the mitochondria-derived peptide humanin, has demonstrated protective effects against various cardiovascular diseases. However, the specific pharmacological effects of HNG in heart failure (HF) have not been previously reported. Therefore, in this study, we aimed to investigate the potential protective effect of HNG in HF using a mouse model. HF was induced in mice through intraperitoneal injection of isoproterenol or transverse aortic constriction, followed by separate administration of HNG to assess its therapeutic impact. Our results revealed that HNG treatment significantly delayed the onset of cardiac dysfunction and structural remodeling in the HF mouse model. Furthermore, HNG administration was associated with reduced infiltration of inflammatory cells, improved myocardial fibrosis, and attenuation of cardiomyocyte apoptosis in the treated cardiac tissues. Additionally, we identified the involvement of the transforming growth factor-beta signaling pathway in the beneficial effects of HNG in isoproterenol-induced HF mice. Collectively, these findings underscore the therapeutic potential of HNG in preventing the progression of HF, as demonstrated in two distinct HF mouse models.

1. Background

Heart failure (HF) is a chronic ailment, representing the culmination of diverse cardiovascular disorders. Numerous intricate mechanisms contribute to its progression, including remodeling of energy metabolism, myocardial fibrosis, apoptosis, and infiltration of inflammatory cell [1]. Despite notable therapeutic advancements, current medications merely slow down HF progression. The primary objective in managing HF patients is the restoration of cardiac pump function. Within the cell, mitochondria serve as the vital "pumps" by supplying the heart with most of its energy through oxidative phosphorylation. Remarkably, amidst the multifaceted development of HF, emerging evidence underscores the inevitable role of mitochondrial dysfunction in its progression. The role of mitochondrial dysfunction in the development of HF encompasses various aspects, including abnormal metabolic substrate utilization, impaired mitochondrial oxidative phosphorylation, increased reactive oxygen species, and aberrant mitochondria quality control [2]. Additionally, mitochondria possess their own independent genome known as mitochondrial DNA (mtDNA), which collaborates with

* Corresponding author. Department of Cardiology, The Second Affiliated Hospital of Chongqing Medical University, No. 288 Tianwen Avenue, Nan'an District, Chongqing, 401336, China.
E-mail address: sulicq@163.com (L. Su).
[1] Q. Zhao and M. Cai contributed equally to this work.

https://doi.org/10.1016/j.heliyon.2023.e21892
Received 3 January 2023; Received in revised form 18 September 2023; Accepted 31 October 2023
Available online 8 November 2023

the transcription and translation processes of nuclear genome to regulate mitochondrial function [3].There is growing evidence suggesting that mtDNA plays a crucial role in the metabolic and functional changes observed in the heart [4–6]. In summary, mtDNA is implicated in the progression of HF.

The first discovered mitochondrial-derived peptide, humanin, consists of 24 amino acids [7]. It is encoded by a small open reading frame within the 16S ribosomal RNA coding region of mtDNA. Humanin 's initial identification occurred in 2001 during the screening of a cDNA library derived from the brain tissue of a patient diagnosed with familial Alzheimer's disease [8]. Subsequent studies have revealed the presence of humanin in a diverse range of organs and tissues, including the heart, kidneys, liver, testes, skeletal muscles, and brain [9]. Although the precise mechanism of action of humanin remains to be fully elucidated, it has been established that humanin plays a significant role in the reverse communication process between the mitochondria and the nuclear genome, thereby contributing to the maintenance of cellular homeostasis and integrity [10]. This critical involvement in cellular function has led to the confirmation of humanin's protective role in various diseases and experimental models, including Alzheimer's disease [8,11,12], cardiovascular diseases [13,14], stroke [15,16] and type 2 diabetes mellitus [17].

One notable humanin analogue is S14G-humanin (HNG), in which glycine replaces Ser14. Previous research has demonstrated that chronic administration of HNG can effectively prevent age-related myocardial fibrosis in mice [18]. Furthermore, HNG has been found to exert protective effects against myocardial injury in mouse models of diabetes [19]. Additionally, in both mouse and pig models of myocardial ischemia and reperfusion, HNG has exhibited cardioprotective properties by mitigating resulting cardiac dysfunction [20, 21]. These findings unequivocally highlight the therapeutic potential of HNG in preserving cardiac function across diverse injury conditions.

Building upon the established evidence of HNG's ability to improve cardiac function under conditions of oxidative stress, our study aimed to investigate the protective role of HNG in a mouse model of HF. We hypothesized that HNG could have a beneficial effect on HF by mitigating the adverse cardiac remodeling and dysfunction associated with this condition. To evaluate this hypothesis, we utilized an isoproterenol (ISO)-induced mouse model of HF and examined the underlying downstream signaling mechanisms. Furthermore, we reconfirmed the protective effect of HNG on HF using a mouse model of aortic constriction (TAC)-induced HF.

By conducting these experiments and analyzing the potential signaling mechanisms involved, our investigation aimed to enhance our comprehension of the cardioprotective effects of HNG in the context of HF.

2. Material and methods

2.1. Animals and reagents

To establish the mouse models of HF induced by TAC and ISO, eight-week-old C57BL/6J mice weighing 20–25 g were procured from Chengdu Ensville Biotechnology Co., LTD. The mice were maintained at the specific pathogen-free level and housed in cages with 5–6 mice per cage. They were provided with ad libitum access to food and water, without any restrictions. The mice were subjected to a 12-h day-night alternating environment, with a temperature of 24 °C and a relative humidity ranging from 40 % to 50 %. ISO was procured from the Sigma Company in the United States. The synthetic peptide HNG, comprising a total of 24 amino acids (Met-Ala-Pro-Arg-Gly-Phe-Ser-Cys-Leu-Leu-Leu-Leu-Thr-Gly-Glu-Ile-Asp-Leu-Pro-Val-Lys-Arg-Arg-Ala), was obtained from Chengdu YoungShe Chemical Co., Ltd in China with a purity of $\geq$95 %. Prior to conducting any animal experiments, all protocols were approved by the Ethics Committee of Experimental Animal of West China Hospital of Sichuan University.

2.2. Study design

Eight-week-old healthy adult male C57BL/6 mice weighing 20–25g were randomly assigned to two groups: the ISO group and the control group. Mice in the ISO group received intraperitoneal injections of ISO at a dose of 60 mg/kg. In contrast, mice in the control group were administered the same volume of normal saline via intraperitoneal injection. This treatment regimen was continued for a duration of 28 days. Following the administration of ISO, a subset of mice from the ISO group was randomly chosen to receive intraperitoneal injections of HNG at a dosage of 4 mg/kg, a dose selected based on previous studies demonstrating the cytoprotective effects of HNG in mouse models [18]. This subset of mice formed the treatment group. A total of 55 mice were included in this study, divided into three groups: a control group (n = 8), an ISO group (n = 23), and an HNG group (n = 24). After the 28-day experimental period, the survival rates were as follows: 8 mice survived in the control group, 7 mice survived in the ISO group, and 13 mice survived in the HNG group. To evaluate cardiac function, echocardiogram was performed on day 14 and day 28 after the administration of ISO in all three groups. To establish a mouse model of HF induced by pressure overload, adult male C57BL/6 mice weighing 20–25g were randomly divided into two groups: the TAC group and the sham group. TAC group mice were anesthetized with 1.5 % isoflurane and underwent a thoracotomy. The aortic arch was dissected away from the surrounding muscle and soft tissue. A 6-0 silk thread was passed under the aorta using a homemade wire guide. Then, a 27-gauge needle (0.40 mm) was placed beside the aortic arch, ligated together, and excised. Sham group mice underwent the same procedure except for aortic constriction. Two weeks after the establishment of the pressure-induced HF mouse model, the mice were randomly divided into a postoperative treatment group (TAC + HNG) and a sham treatment group (Sham + HNG), with treatment of HNG of 4 mg/kg. In this HF mouse model, ultrasound imaging of the aortic arch was performed on postoperative day 3. Subsequently, echocardiography was conducted at postoperative weeks 2, 4, 6, and 8 on the TAC group, the sham group, the sham treatment group (Sham + HNG), and the postoperative treatment group (TAC + HNG). A total of 14 mice were randomly assigned, with 6 mice in the sham group and 8 mice in the TAC group. However, one mouse in the TAC group died within 3 days, and another mouse did not show cardiac function decline on day 14. Therefore, the remaining 6

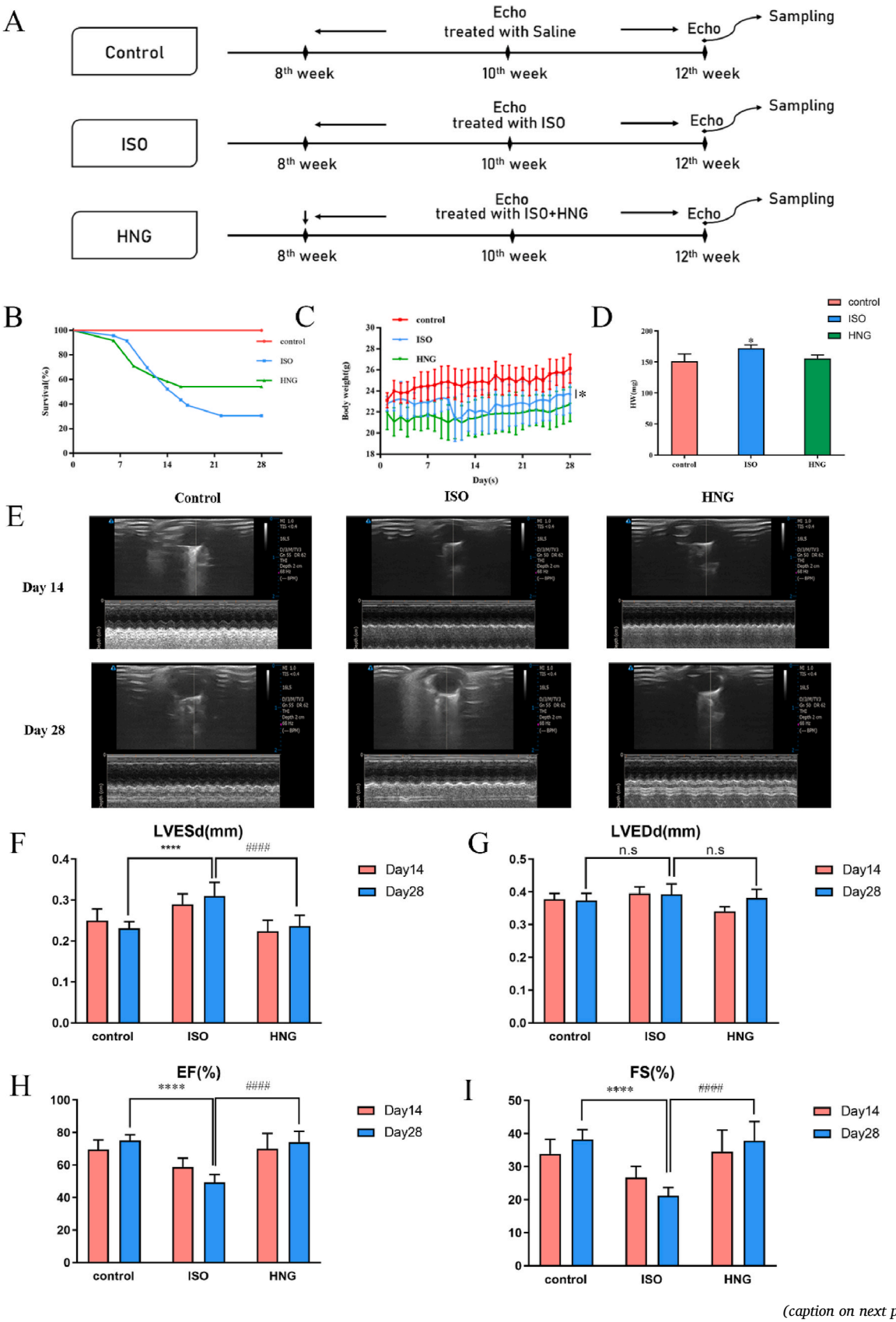

(caption on next page)

Fig. 1. Effects of HNG on the general condition of ISO-induced HF mice. A: Schematic diagram of the experiment flow in ISO mice. B: The 28-day survival curve of mice. C: Body weight changes of mice for 28 days. *P < 0.05 ISO vs Con, mean ± SEM, n = 8 for Con, 7 for ISO, 13 for HNG. D: The heart weight of mice at 28 days. *P < 0.05 ISO vs Con, #p < 0.05 HNG vs ISO, mean ± SEM, n = 3 for each group. E: Representative images of mice echocardiography at day 14 and 28. F–I: Echocardiographic measurements of F) left ventricular end-systolic dimension (LVESd, mm); G) left ventricular end-diastolic dimension (LVEDd, mm); H) Ejection Fraction (EF, %); I) Fractional Shortening (FS, %). *p < 0.05, **p < 0.01, ****p < 0.001 ISO vs Con, #p < 0.05, ##p < 0.01, ####p < 0.001 HNG vs ISO, mean ± SEM, n = 6 for ISO and HNG, n = 3 for Con.

mice in the TAC group were further divided into the postoperative treatment group (TAC + HNG).

2.3. Echocardiography

Mice were anesthetized with 1.5 % isoflurane, and their limbs were then fixed on the operating table. Images were acquired in the short-axis section at the level of sternocleidomastoid muscle and the long-axis section at the level of mitral valve using a 13 MHz high-frequency probe. We measured the following parameters left ventricular end-systolic diameter (LVESd), left ventricular end-diastolic diameter (LVEDd), ejection fraction (EF), left ventricular short-axis shortening rate (FS), end-systolic volume (ESV) and end-diastolic volume (EDV).

2.4. Histopathological analysis

Heart tissues of mice were fixed in 10 % neutral formalin, embedded in paraffin, then serially cut in 4 μm sections. Cardiac morphology was assessed using hematoxylin and eosin (H&E) staining, cardiac collagen content was evaluated by Sirius red staining. The extent of myocardial fibrosis was analyzed using ImageJ software. Three fields of view were randomly selected, and each group included at least three independent samples. All histological analyses were performed in a blinded manner.

2.5. Immunofluorescence assay

Heart sections were incubated with Trias Red-X-conjugate wheat germ agglutinin (WGA-Texas Red) (W21405, Invitrogen, USA) to observe and measure the cross-sectional area of cardiomyocytes. TUNEL (KGA7071, KeyGEN Biotech, China) was used to assess cardiomyocyte apoptosis. Leica DM4000B fluorescence microscope was used to obtained images of section. To determine the number of apoptotic cells, three fields were randomly selected, and using ImageJ software, the entire membrane of at least 100 cells was evaluated from each sample. Each group included at least three independent samples.

2.6. Western blot analysis

The proteins from heart tissues were divided. Primary antibodies used included p44/42 MAPK (Erk1/2) (1:1000; 4695, Cell Signaling Technology, USA), Phospho-p44/42 MAPK (Erk1/2) (Thr202/Tyr204) (1:1000; 4370, Cell Signaling Technology, USA), SAPK/JNK (1:1000; 9252, Cell Signaling Technology, USA), Phospho-SAPK/JNK (Thr183/Tyr185) (1:1000; 4668, Cell Signaling Technology, USA), p38 MAPK (1:1000; 8690, Cell Signaling Technology, USA), Phospho-p38 MAPK (Thr180/Tyr182) (1:1000; 4511, Cell Signaling Technology, USA), Smad2 (1:500; 5339, Cell Signaling Technology, USA), Phospho-Smad2 (Ser465/Ser467) (1:500; 18338, Cell Signaling Technology, USA), Smad2/3 (1:1000; 8685, Cell Signaling Technology, USA), Phospho-Smad2 (Ser465/467)/Smad3 (1:1000; Ser423/425) (8828, Cell Signaling Technology, USA), TGF-β (1:500; 3709, Cell Signaling Technology, USA), and GAPDH (1:1000; 2118, Cell Signaling Technology, USA). The secondary antibody used for immunoblotting was Anti-rabbit IgG, HRP-linked Antibody (1:3000; 7074, Cell Signaling Technology, USA).

2.7. Serum analysis

We use an ELISA kit (Elabscience Biotechnology Co., Ltd, China) for the N-terminal pro-B type natriuretic peptide (NT-proBNP) to measure the concentration of serum NT-proBNP in each serum sample according to the manufacturer's instructions.

2.8. Statistical analysis

GraphPad Prism 9 software was used for data result analysis. The Shapiro–Wilk test was used to evaluate the normality of the data distribution. For normally distributed data, one-way analysis of variance was used to assess significance. For non-normally-distributed data, the Mann–Whitney *U* test was used for analysis. $P < 0.05$ was considered statistically significant.

3. Results

3.1. HNG alleviates the general condition of ISO-induced HF mice

To establish HF mouse model, mice were intraperitoneally injected with ISO of 60 mg/kg/day for 28 consecutive days. HNG group

received an additional treatment of HNG of 4 mg/kg (Fig. 1A). After daily intraperitoneal injection of ISO, the mice exhibited various catecholamine effects, including prominent signs of mania, increased movement, and piloerection, followed by a general sense of malaise after approximately 5 min. This phenomenon can be attributed to physical exhaustion, as indicated in Supplement A. Both the

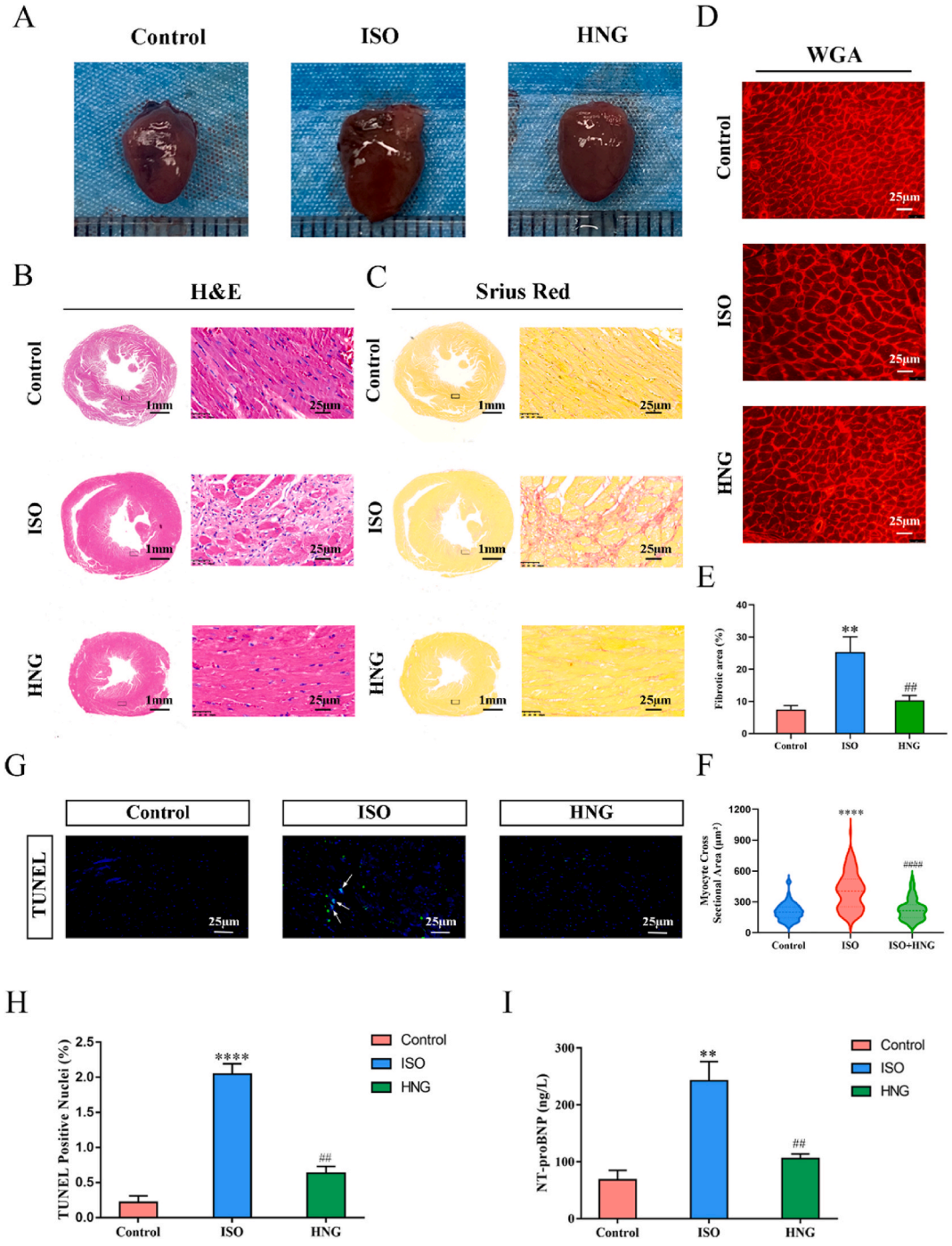

Fig. 2. Effect of HNG on myocardial morphology in ISO-induced HF mice. A: Overall view of the heart 28 days after ISO injection. B: H&E staining of the cross section of the heart. C: Sirius Red staining of the cross section of the heart. D: WGA staining for cross-sectional area of cardiomyocyte. E: Quantitative analysis of the fibrotic area (%), n = 3 for each group. F: Quantitative analysis of the myocyte cross-sectional area (μm2). G: TUNEL assay for detecting the myocardial apoptosis. H: Quantitative analysis of myocardial apoptosis. ****p < 0.001 ISO vs Con, ##p < 0.01 HNG vs ISO, mean ± SEM, n = 3 for each group. I: ELISA assay for heart failure maker of NT-proBNP (ng/L). **p < 0.01 ISO vs Con, ##p < 0.01 HNG vs ISO, mean ± SEM, n = 3 for each group.

ISO and HNG mice started to exhibit mortality from day 6 after intraperitoneal ISO injection. The mortality peak in the ISO group occurred on the 11th and 14th days, while the mortality peak in the HNG group occurred on the 9th day. However, after the peak mortality period, the HNG group showed a significantly lower mortality rate compared to the ISO group, and no mice died from day 16 to the end of the experimental period. In contrast, mice in the ISO group continued to experience mortality after the peak until day 22 (Fig. 1B).

Furthermore, a cliff-like weight loss was observed in ISO group on day 11, coinciding with the peak time of mortality. After the peak of death on day 14, the body weight gradually recovered from day 15 (Fig. 1C). Similarly, mice in the HNG group showed a small weight loss on days 8, 9, and 10, followed by a gradual weight gain. Ultimately, compared to the beginning of the experiment, the ISO and HNG group showed slight difference in body weight, whereas the control group maintained a steady increase. On day 28, the mice in the ISO group had a heart weight that was higher than the mice in the control group, and they also exhibited marked alopecia (Supplement B). In contrast, the HNG group showed improvement, with a heart weight lower than the ISO group (Fig. 1D).

3.2. Effect of HNG on cardiac function in ISO-induced HF mice

Echocardiography was conducted on day 14 and 28 to assess the impact on left ventricular cardiac function. The ISO group exhibited impaired cardiac function, which was ameliorated by HNG treatment (Fig. 1E). Specifically, LVESd in the ISO group displayed a significant increase of 16 % and 30 % after continuous ISO injection for 14 and 28 days, respectively, in comparison to the control group (Fig. 1F). However, the HNG group exhibited preserved LVESd without a substantial increase. To further evaluate systolic function, the ESV was calculated. The ISO group demonstrated a significant increase of 52 % on day 14, which further escalated to 139 % by day 28, in contrast to the control group. In contrast, the HNG group displayed only a 10 % increase compared to the control group at day 28 (Supplement D). Additionally, the ISO group exhibited a decline of 22 % and 35 % in LVEF on day 14 and 28, respectively, compared to the control group. Conversely, the HNG group did not exhibit significant changes in LVEF when compared to the control group (Fig. 1H). The FS in the ISO-injected mice decreased by 22 % and 45 % on days 14 and 28, respectively, in comparison to the control group, whereas the HNG group displayed minimal differences compared to the control group (Fig. 1I). However, no notable effects on cardiac diastolic function were observed following ISO injection (Fig. 1G), and similarly, EDV demonstrated negligible changes (Supplement C).

3.3. Effect of HNG on myocardial morphology in ISO-induced HF mice

On day 28, all mice were euthanized under anesthesia following echocardiography. Upon dissection, it was observed that the hearts of control mice exhibited normal gross morphology, with relatively intact geometric morphology, good elasticity and toughness. However, the hearts of mice injected with ISO for 28 days maintained their geometric integrity but displayed a significantly increased in size and accompanied by a dark red coloration. Moreover, the elasticity and toughness of the hearts exhibited varying degrees of reduction. In comparison, the hearts of HNG-treated mice showed superior characteristics compared to the ISO mice in terms of size, color, elasticity, and toughness. However, they exhibited a darker pigmentation and marginally larger volume compared to the control mice (Fig. 2A).

After dissecting each group of mice, the hearts were sectioned for H&E staining. Analysis of the stained sections revealed that in control mice, the myocardial cells were neatly arranged, and the myocardial fibers exhibited a parallel arranged and tightly structured pattern. The fibers appeared as bundles with clear horizontal stripes. The nuclei of the cells were clearly visible and exhibited normal shape and size. There were no signs of cell edema, degeneration, necrosis, or inflammatory cell infiltration observed among the cells. Conversely, the H&E-stained sections of mice from the ISO group revealed significant pathological changes. Cardiomyocytes exhibited hypertrophy, along with evidence of edema and cytoplasmic looseness, characterized by the presence of numerous vacuoles. The cells exhibited variability in shape, size, and contour. The myocardial fibers appeared disrupted, swollen, disordered, and partially disappeared. Notably, there was a relatively noticeable infiltration of inflammatory cells observed between the cardiomyocytes. In contrast, the HNG-treated mice displayed varying degrees of improvement in cardiomyocyte swelling, cell arrangement structure, and inflammatory cell infiltration (Fig. 2B). Sirius red staining of the ISO group revealed a substantial deposition of collagen, interstitial fibrosis, atrophy or hypertrophy of peripheral cardiomyocytes, and vacuolization of some myocardial fibers. These pathological changes were particularly prominent in the endocardial region after continuous ISO injection for 28 days (Fig. 2C, E). WGA fluorescence staining and semi-quantitative analysis of myocardial cross-sectional area in the ISO group demonstrated a significant increase in myocardial cross-sectional area, indicating cardiac hypertrophy. Conversely, these phenomena were significantly improved in the hearts of HNG-treated mice (Fig. 2D, F).

Given that the cardiac function of mice had reached an obvious decompensated stage in the later phase, hypertrophic cardiomyocytes were unable to provide continued compensatory ability for cardiac ejection. Prolonged overload eventually resulted in cardiomyocyte loss, transitioning from the compensatory stage to the decompensated stage. Apoptosis represents one of the most common forms of myocardial death. Therefore, TUNEL staining was employed to detect apoptosis. The results showed a significant increase in cardiomyocyte apoptosis in the hearts of mice injected with ISO for 28 consecutive days compared to control mice and HNG-treated mice (Fig. 2G and H).

To assess the severity of HF, serum NT-proBNP levels were measured. NT-proBNP, with its longer half-life and greater stability in serum, serves as a reliable indicator of HF severity in clinical practice. Serum samples from each experimental group were collected for NT-proBNP detection (Fig. 2I). The results indicated that the ISO group exhibited NT-proBNP levels 3.35 times higher than those of the control group. Although the HNG-treated mice exhibited NT-proBNP levels 1.69 times higher than those of the control group, the

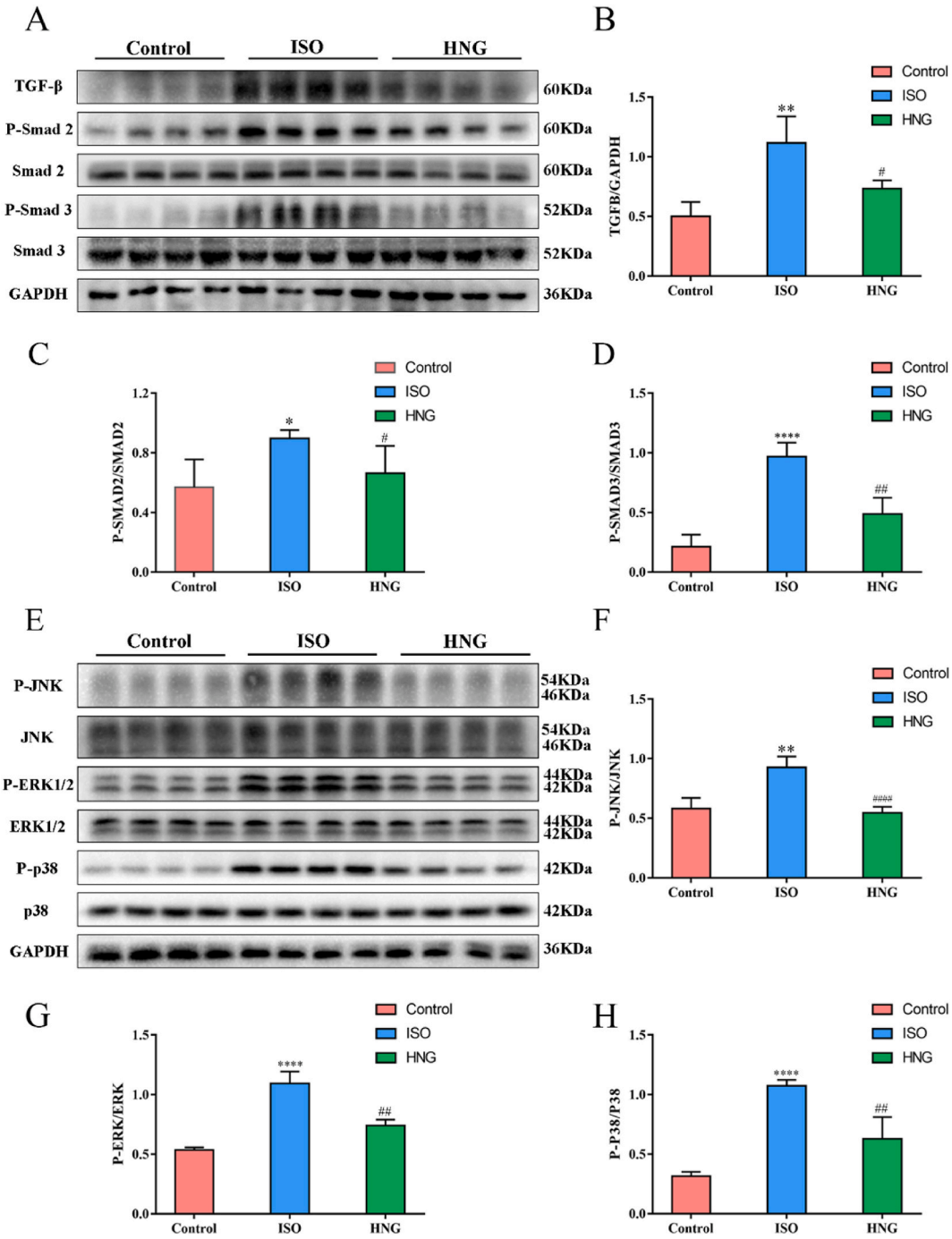

Fig. 3. Effect of HNG on fibrotic pathway in ISO-induced HF mice. A: Western blot analysis for key molecules of TGF-β signaling pathway in TGF-β, total Smad2, P-Smad2, total Smad3, P-Smad3. Quantitative analysis of expression in B) TGF-β. **P < 0.01 ISO vs Con, #p < 0.05 HNG vs ISO; C) Smad2, P-Smad2. *p < 0.05 ISO vs Con, #p < 0.05 HNG vs ISO; D) Smad3, P-Smad3. ****P < 0.001 ISO vs Con, ##p < 0.01 HNG vs ISO, mean ± SEM, n = 4 for each group. E: Western blot analysis for key molecules of MAPK signing pathway. Quantitative analysis of expression in F) JNK, P-JNK. **p < 0.01 ISO vs Con, ####p < 0.001 HNG vs ISO; G) ERK, P-ERK. ****p < 0.001 ISO vs Con, ##p < 0.01 HNG vs ISO; H) p38, P-p38. ****p < 0.001 ISO vs Con, ##p < 0.01 HNG vs ISO, mean ± SEM, n = 4 for each group.

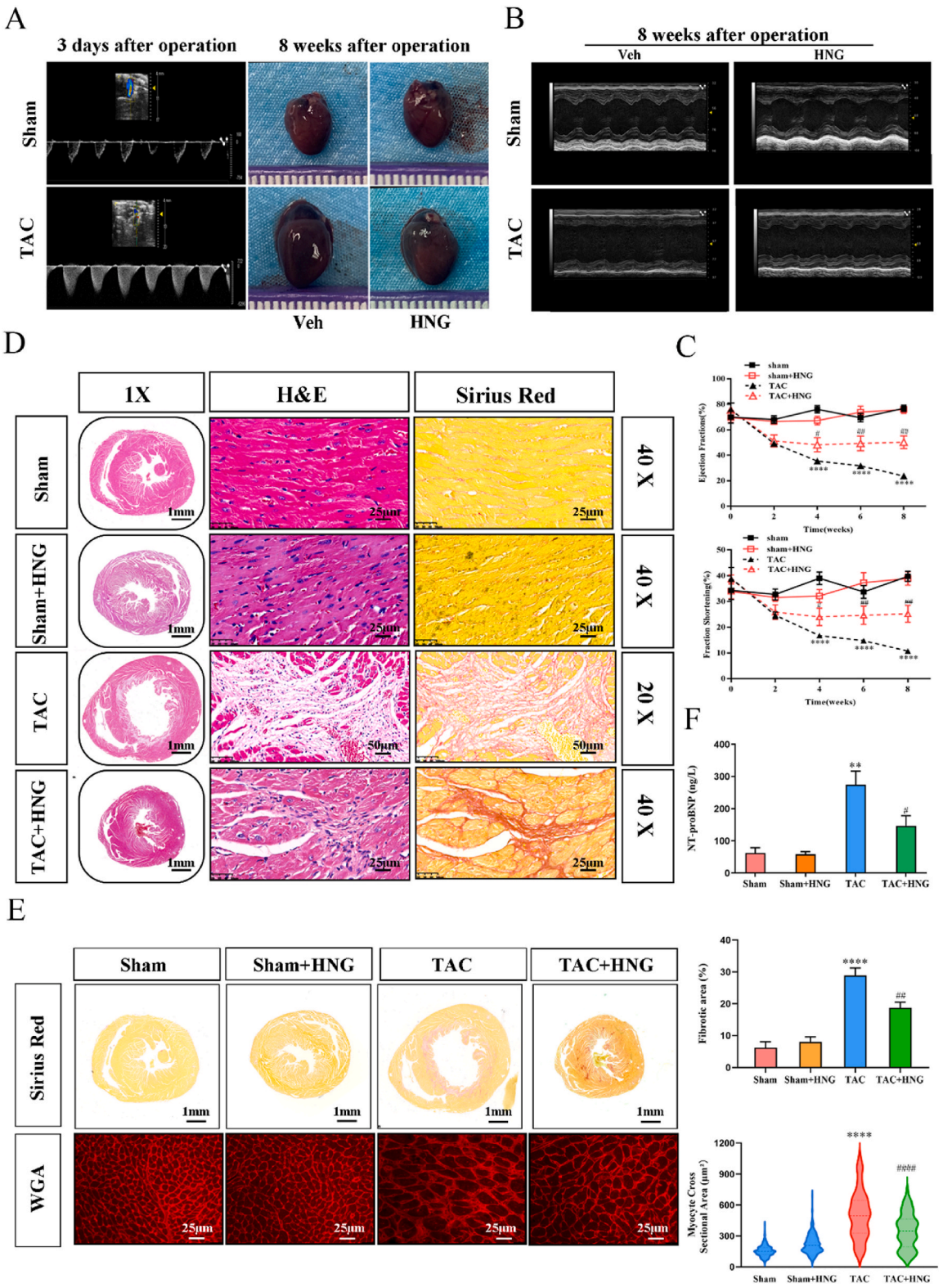

Fig. 4. Effect of HNG in TAC-induced HF mice. A: Aortic arch blood flow velocity in mice on 3 days after TAC surgery & overall view of the heart at 8 weeks after TAC operation. B: Representative images of mice echocardiography at 8 weeks after TAC operation. C: Progressive percent of left ventricular ejection fraction (LVEF). ****P < 0.001 Sham vs TAC, #p < 0.05, ##p < 0.01, TAC + HNG vs TAC; progressive percent of fraction shortening (FS), ****P < 0.001 Sham vs TAC, #p < 0.05, ##p < 0.01 TAC + HNG vs TAC, mean ± SEM, n = 3 for each group. D–E:

Histopathological analysis of overall view for heart size, H&E staining for cross sectional view of hearts and cardiac structure, Sirius Red stating for interstitial fibrosis, and WGA stating for cross-sectional area of cardiomyocytes. Quantitative analysis of the fibrotic area (%), n = 3 per group. Quantitative analysis of the myocyte cross-sectional area (μm2). F: NT-proBNP in serum by ELISA. **P < 0.01 TAC vs Sham; #p < 0.05 TAC + HNG vs TAC, mean ± SEM, n = 3 for each group.

values were significantly lower than those of the ISO group.

3.4. Effect of HNG on fibrotic pathway in ISO-induced HF mice

After observing myocardial fibrosis in the mice hearts, we further investigated the levels of fibrosis-related proteins, such as TGF-β, and its downstream effectors Smad2 and Smad3, as well as the phosphorylated forms of Smad2 (Ser465/467) and Smad3 (Ser423/Ser425) (Fig. 3A). Concurrently, we investigated the MAPK family proteins, including P38, ERk1/2 and JNK, along with the phosphorylation of P38 Thr180/Tyr182 (p-p38), ERK1/2 Thr202/Tyr204 (p-ERK1/2), and JNK Thr183/Tyr185 (p-JNK) (Fig. 3E). We observed a significant increase in TGF-β levels in the myocardial tissue of mice injected with ISO for 28 days, accompanied by the activation of downstream effector molecules, Smad2 and Smad3. Moreover, molecules in the MAPK family were also activated. However, in comparison to the ISO group, mice treated with HNG displayed significantly decreased levels of these related proteins. These findings suggest that HNG inhibit myocardial fibrosis in mice by suppressing TGF-β-related pathways and MAPK family molecules.

3.5. Effect of HNG in TAC-induced HF mice

The chronic ISO-induced HF mouse model is widely acknowledged for its ease of establishment and its ability to simulate advanced HF in humans [22]. However, chronic adrenergic stimulation is just one contributing factor in HF development. In contrast, the TAC model, which replicates left ventricular pressure overload, is considered a more reliable mouse model for HF studies [23]. To further validate the cardioprotective effects of HNG observed in the ISO-induced HF mouse model, we conducted TAC surgery to induce pressure overload in mice. By utilizing this additional experimental approach, we aimed to confirm the reproducibility of HNG's beneficial effects in a different HF model context (Supplement E). TAC-induced HF mouse models were established as described in the methods, and the blood flow velocity was measured using aortic arch ultrasound on the third day after the surgery to confirm the success of the procedure (Fig. 4A). Two weeks post-surgery, the mice were randomly divided into two groups. One group received a daily dose of HNG at 4 mg/kg, while the other group received an equivalent volume of normal saline. Cardiac function was monitored at 2-, 4-, 6- and 8-week post-operation (Fig. 4B). The echocardiograms provided an overall assessment of cardiac function in the mice with pressure overload, showcasing the transition from a compensatory state to a decompensated state over time (Fig. 4C). In the TAC group, EF decreased by 26 % on day 14 compared to the Sham group. Subsequently, EF continued to decrease by 14 %, 5 %, and 8 % at weeks 4, 6, and 8, respectively. Similarly, FS decreased by 14 % on day 14 and continued to decline by 8 %, 4 %, and 4 % at weeks 4, 6, and 8, respectively, compared to the Sham group (Fig. 4C).

After 8 weeks, mice were dissected, serum samples were collected to measure the levels of NT-proBNP. The NT-proBNP levels in the TAC group was significantly elevated compared to the other three groups. Although the mice in the TAC + HNG group exhibited significantly lower NT-proBNP levels compared to the TAC group, their levels were still higher than those observed in the Sham group and the Sham + HNG group. Notably, there was no significant difference in serum NT-proBNP levels between the sham group and the Sham + HNG group (Fig. 4F).

Furthermore, histopathological analysis of the collected heart tissues revealed distinct findings among the four groups. In the TAC group, H&E staining demonstrated a disorganized arrangement of cardiomyocytes, accompanied by cell hypertrophy, edema, and cavitation. Inflammatory cell infiltration and myocardial fiber fragmentation were also observed. Sirius red staining exhibited extensive collagen deposition, indicating significant myocardial fibrosis and perivascular fibrosis (Fig. 4D). Additionally, WGA staining revealed an increase in cardiomyocyte cross-sectional area (Fig. 4E). In the TAC + HNG group, histopathological sections displayed varying degrees of improvement in the aforementioned conditions. However, some degree of fibrosis was still present compared to the Sham and Sham + HNG groups. In comparison, the Sham group and the Sham + HNG group exhibited no signifi cant differences in their histopathological characteristics. Moreover, we investigated the levels of fibrosis-related proteins and MAPK family proteins, the results also suggested that HNG interrupting the process of myocardial fibrosis in TAC mice by suppressing TGF-β-related pathways and MAPK family molecules (Supplement 2).

In conclusion, the administration of HNG effectively prevented the progression of HF in mice induced by TAC. Cardiac function did not further deteriorate following the initiation of HNG treatment, although complete reversal of cardiac dysfunction was not achieved. The Sham + HNG group demonstrated that infusion of HNG alone did not pose an observable safety risk to mice.

4. Discussion

The prevention and treatment of HF are challenging tasks, requiring innovative therapeutic approaches to enhance the quality of life and long-term prognosis of HF patients [24]. Humanin, a 24-nucleotide peptide encoded by the 16S ribosomal RNA of mtDNA [25], has been shown to exhibit high activity when serine residues at 14 amino acid positions are substituted with glycine, resulting in the generation of HNG. Over the past decade, the roles of humanin and its derivatives have been extensively investigated in various

biological processes, including cell apoptosis, cell survival, substrate metabolism, inflammatory responses, as well as the response to oxidative stress, ischemia, and starvation stressors [26,27]. In this study, we evaluated the effects of intraperitoneal injection of HNG on the development of HF in mice under conditions of chronic adrenergic stimulation and chronic pressure overload. Our findings demonstrated that HNG treatment significantly delayed the development of cardiac dysfunction and structural remodeling in the mouse model of HF. Additionally, reduced infiltration of inflammatory cells, improved myocardial fibrosis, and attenuation of myocardial cell apoptosis were observed in the cardiac tissues treated with HNG. Furthermore, we highlighted the importance of the cardiac fibrosis pathway in the effect of HNG on mice under conditions of chronic adrenergic stimulation. Therefore, our study demonstrates the therapeutic potential of HNG in preventing the development of HF in two distinct mouse models.

Recent investigations have yielded compelling evidence supporting the protective properties of humanin in various cardiovascular disorders, including atherosclerosis, acute myocardial infarction, myocardial ischemia-reperfusion injury, and myocardial aging [28]. The consistent underlying mechanism behind these protective effects involves the modulation of oxidative stress. For instance, a study utilizing a rat model of preterm birth demonstrated significant alterations in the structure and function of the cardiac left ventricle mitochondria following transient neonatal exposure to hyperoxia [29]. These alterations encompassed a reduction in mitochondrial size and integrity, along with a subsequent decline in oxidative phosphorylation capacity later in life. Additionally, in their investigation comparing young adults born preterm with those born full-term, the researchers established an association between humanin levels and EF. Furthermore, it has been shown that exogenous treatment with HNG mitigates myocardial fibrosis and apoptosis in aging mice [18]. Moreover, compelling evidence supports the efficacy of exogenous humanin in restoring cardiac function across a range of experimental models. Prior studies have provided evidence showcasing the cardioprotective effects of HNG in both mouse and porcine models of myocardial ischemia-reperfusion injury, including a decrease in infarct size and significant improvement in LV function [20,21]. Additionally, HNG has been shown to ameliorate cardiac dysfunction induced by both streptozotocin [19] and doxorubicin [30]. In our present study, we provide compelling evidence that treatment with HNG effectively improves cardiac function in mice with HF induced by ISO and TAC. These findings further emphasize the therapeutic potential of exogenous HNG as a promising strategy for treating HF and restoring overall cardiac function.

TGF-β is a prominent fibrogenic growth factor that has been extensively implicated in the pathological progression of cardiac fibrosis. Numerous studies have revealed that TGF-β participates in the development of ventricular fibrosis, as evidenced by its overexpression and constitutive expression of activating mutant TGF-β protein in cardiomyocytes. The activation of TGF-β subsequently triggers a cascade of intracellular effector proteins, particularly the Smad protein family. Both in vivo and in vitro investigations have demonstrated that activation of either the canonical Smad-dependent signaling pathway or the non-canonical Smad-independent signaling pathway can promote fibroblast activation in the fibrotic heart [31,32]. In our study, we examined the expression of TGF-β in myocardial tissue of mice treated with ISO for 28 consecutive days to induce HF. We observed activation of TGF-β in the heart tissue of these mice and subsequently assessed the activation of the canonical Smad-dependent pathway through phosphorylation of Smad2 and Smad3. We found that the expression of TGF-β was decreased in mice treated with HNG compared to the HF group. Moreover, the phosphorylation and activation of downstream signaling pathways was also reduced. These results indicate that HNG may inhibit cardiac fibrosis by suppressing the activation of the TGF-β-Smad2/3 pathway, thereby protecting cardiac function in mice.

Mitochondria, as vital organelles in cells, not only serve as the primary energy source for cardiomyocytes but also play essential roles in various biological processes, such as the generation of ROS, calcium homeostasis, cell survival, and apoptosis [33,34]. Moreover, they play a significant regulatory role in cardiac fibrosis [35]. Pathological factors such as ischemia-reperfusion injury, hormonal imbalance, and chronic pressure overload can lead to mitochondrial dysfunction in cardiomyocytes, accelerating cell death. This, in turn, creates a stressful environment and drives the heart into a vicious cycle, eventually leading to irreversible HF. Humanin, a peptide derived from mtDNA, has been shown to exhibit reduced levels in circulation and cardiac tissues in various diseases [13,36,37], suggesting its potential role in protecting the heart and maintaining cardiac function during HF development. Our study, through the external supplementation of HNG, demonstrates the improvement of pathological changes and consequent protection of cardiac function, thus confirming this role. Previous research suggests that humanin's protective function may be exerted through various processes, including its impact on mitochondrial structure and function [38–40], leading to the improvement of ROS generation, mitochondrial dynamics, and mitochondrial-induced cell apoptosis [41–44]. Additionally, it may act as a signaling molecule to enhance communication between mitochondria or between mitochondria and the cell nucleus [45,46]. Furthermore, our study suggests that HNG may improve cardiac fibrosis by inhibiting the fibrotic pathway TGF-β activation.

It should be noted that our study has a limitation in that we did not verify the specific effects of HNG on different cell types in the heart in vitro, which represents a limitation in understanding the cellular mechanisms underlying its actions. Moreover, as humanin is one of the mitochondria-derived peptides, it is crucial to investigate the extent to which exogenous supplementation of HNG affects mitochondrial function and morphology. This aspect remains to be fully elucidated and will be a key focus of our future research endeavors.

In conclusion, our study provides evidence for the protective effect of HNG on cardiac function in mouse models of HF induced by ISO and TAC. The underlying mechanism involves the inhibition of TGF-β-Smad2/3 pathway activation. These findings underscore the potential therapeutic application of HNG in the treatment of cardiac insufficiency. Further research is necessary to validate these findings and explore the comprehensive therapeutic potential of HNG in managing cardiac dysfunction.

Declarations

The present article is a work of originality, authored by the individuals explicitly mentioned, all of whom possess a comprehensive

understanding of its content and have provided their consent for its submission. The present article has not been published previously, it is not under consideration for publication elsewhere.

Ethics approval/Consent to participate

All protocols of this study were approved by the Ethics Committee of Experimental Animal of West China Hospital of Sichuan University (20220530005).

Funding

This work was supported by the National Natural Science Foundation of China (NSFC 8197020688).

Availability of data and material

Data will be made available on request.

Code availability

Not applicable.

Author contribution

Q.Z., M.C., D.L, B.Z, and S.Z. designed and performed the experiments, analyzed data, and prepared the manuscript; Z.W. provides suggestions on tissue staining technique; Y·S and L.S. designed the experiments, reviewed the data, and provide critical suggestions.

Declaration of competing interest

The authors declare that they have no known competing financial interests or personal relationships that could have appeared to influence the work reported in this paper.

Appendix A. Supplementary data

Supplementary data to this article can be found online at https://doi.org/10.1016/j.heliyon.2023.e21892.

References

[1] T. Tuomainen, P. Tavi, The role of cardiac energy metabolism in cardiac hypertrophy and failure, Exp. Cell Res. 360 (1) (2017) 12–18.
[2] D. Sacks, B. Baxter, B.C.V. Campbell, J.S. Carpenter, C. Cognard, D. Dippel, et al., Multisociety consensus quality improvement revised consensus statement for endovascular therapy of acute ischemic stroke, Int. J. Stroke 13 (6) (2018) 612–632.
[3] O. Matilainen, P.M. Quirós, J. Auwerx, Mitochondria and epigenetics - crosstalk in homeostasis and stress, Trends Cell Biol. 27 (6) (2017) 453–463.
[4] T. Oka, S. Hikoso, O. Yamaguchi, M. Taneike, T. Takeda, T. Tamai, et al., Mitochondrial DNA that escapes from autophagy causes inflammation and heart failure, Nature 485 (7397) (2012) 251–255.
[5] Y. Cao, L. Vergnes, Y.-C. Wang, C. Pan, K. Chella Krishnan, T.M. Moore, et al., Sex differences in heart mitochondria regulate diastolic dysfunction, Nat. Commun. 13 (1) (2022) 3850.
[6] J. Lin, J. Duan, Q. Wang, S. Xu, S. Zhou, K. Yao, Mitochondrial dynamics and mitophagy in cardiometabolic disease, Front Cardiovasc Med 9 (2022), 917135.
[7] D. Coradduzza, A. Congiargiu, Z. Chen, S. Cruciani, A. Zinellu, C. Carru, et al., Humanin and its pathophysiological roles in aging: a systematic review, Biology 12 (4) (2023).
[8] Y. Hashimoto, T. Niikura, H. Tajima, T. Yasukawa, H. Sudo, Y. Ito, et al., A rescue factor abolishing neuronal cell death by a wide spectrum of familial Alzheimer's disease genes and Abeta, Proc Natl Acad Sci U S A 98 (11) (2001) 6336–6341.
[9] M. Bodzioch, K. Lapicka-Bodzioch, B. Zapala, W. Kamysz, B. Kiec-Wilk, A. Dembinska-Kiec, Evidence for potential functionality of nuclearly-encoded humanin isoforms, Genomics 94 (4) (2009) 247–256.
[10] Y. Yang, H. Gao, H. Zhou, Q. Liu, Z. Qi, Y. Zhang, et al., The role of mitochondria-derived peptides in cardiovascular disease: recent updates, Biomed. Pharmacother. 117 (2019), 109075.
[11] T.-Y. Park, S.-H. Kim, Y.-C. Shin, N.-H. Lee, R.-K.C. Lee, J.-H. Shim, et al., Amelioration of neurodegenerative diseases by cell death-induced cytoplasmic delivery of humanin, J. Contr. Release 166 (3) (2013) 307–315.
[12] K. Yen, J. Wan, H.H. Mehta, B. Miller, A. Christensen, M.E. Levine, et al., Humanin prevents age-related cognitive decline in mice and is associated with improved cognitive age in humans, Sci. Rep. 8 (1) (2018), 14212.
[13] A.R. Bachar, L. Scheffer, A.S. Schroeder, H.K. Nakamura, L.J. Cobb, Y.K. Oh, et al., Humanin is expressed in human vascular walls and has a cytoprotective effect against oxidized LDL-induced oxidative stress, Cardiovasc. Res. 88 (2) (2010) 360–366.
[14] Y.K. Oh, A.R. Bachar, D.G. Zacharias, S.G. Kim, J. Wan, L.J. Cobb, et al., Humanin preserves endothelial function and prevents atherosclerotic plaque progression in hypercholesterolemic ApoE deficient mice, Atherosclerosis 219 (1) (2011) 65–73.
[15] X. Xu, K.-W. Chua, C.C. Chua, C.-F. Liu, R.C. Hamdy, B.H.L. Chua, Synergistic protective effects of humanin and necrostatin-1 on hypoxia and ischemia/reperfusion injury, Brain Res. 1355 (2010) 189–194.
[16] A.-L. Cui, J.-Z. Li, Z.-B. Feng, G.-L. Ma, L. Gong, C.-L. Li, et al., Humanin rescues cultured rat cortical neurons from NMDA-induced toxicity not by NMDA receptor, Sci. World J. 2014 (2014), 341529.

[17] R.H. Muzumdar, D.M. Huffman, G. Atzmon, C. Buettner, L.J. Cobb, S. Fishman, et al., Humanin: a novel central regulator of peripheral insulin action, PLoS One 4 (7) (2009), e6334.
[18] Q. Qin, H. Mehta, K. Yen, G. Navarrete, S. Brandhorst, J. Wan, et al., Chronic treatment with the mitochondrial peptide humanin prevents age-related myocardial fibrosis in mice, Am. J. Physiol. Heart Circ. Physiol. 315 (5) (2018) H1127–H1136.
[19] X. Chen, C. Yun, H. Zheng, X. Chen, Q. Han, H. Pan, et al., The protective effects of S14G-humanin (HNG) against streptozotocin (STZ)-induced cardiac dysfunction, Bioengineered 12 (1) (2021) 5491–5503.
[20] R.H. Muzumdar, D.M. Huffman, J.W. Calvert, S. Jha, Y. Weinberg, L. Cui, et al., Acute humanin therapy attenuates myocardial ischemia and reperfusion injury in mice, Arterioscler. Thromb. Vasc. Biol. 30 (10) (2010) 1940–1948.
[21] T.E. Sharp, Z. Gong, A. Scarborough, E.S. Goetzman, M.J. Ali, P. Spaletra, et al., Efficacy of a novel mitochondrial-derived peptide in a porcine model of myocardial ischemia/reperfusion injury, JACC Basic Transl Sci 5 (7) (2020) 699–714.
[22] S.C. Chang, S. Ren, C.D. Rau, J.J. Wang, Isoproterenol-induced heart failure mouse model using osmotic pump implantation, Methods Mol. Biol. 1816 (2018) 207–220.
[23] N.A. Noll, H. Lal, W.D. Merryman, Mouse models of heart failure with preserved or reduced ejection fraction, Am. J. Pathol. 190 (8) (2020) 1596–1608.
[24] E. Tanai, S. Frantz, Pathophysiology of heart failure, Compr. Physiol. 6 (1) (2015) 187–214.
[25] Y. Hashimoto, T. Niikura, Y. Ito, H. Sudo, M. Hata, E. Arakawa, et al., Detailed characterization of neuroprotection by a rescue factor humanin against various Alzheimer's disease-relevant insults, J. Neurosci. 21 (23) (2001) 9235–9245.
[26] Z. Gong, E. Tas, R. Muzumdar, Humanin and age-related diseases: a new link? Front. Endocrinol. 5 (2014) 210.
[27] B. Miller, S.-J. Kim, H. Kumagai, K. Yen, P. Cohen, Mitochondria-derived peptides in aging and healthspan, J. Clin. Invest. 132 (9) (2022).
[28] H. Cai, Y. Liu, H. Men, Y. Zheng, Protective mechanism of humanin against oxidative stress in aging-related cardiovascular diseases, Front. Endocrinol. 12 (2021), 683151.
[29] D. Ravizzoni Dartora, A. Flahault, C.N.R. Pontes, Y. He, A. Deprez, A. Cloutier, et al., Cardiac left ventricle mitochondrial dysfunction after neonatal exposure to hyperoxia: relevance for cardiomyopathy after preterm birth, Hypertension 79 (3) (2022) 575–587.
[30] Y. Lue, C. Gao, R. Swerdloff, J. Hoang, R. Avetisyan, Y. Jia, et al., Humanin analog enhances the protective effect of dexrazoxane against doxorubicin-induced cardiotoxicity, Am. J. Physiol. Heart Circ. Physiol. 315 (3) (2018) H634–H643.
[31] M. Dobaczewski, M. Bujak, N. Li, C. Gonzalez-Quesada, L.H. Mendoza, X.-F. Wang, et al., Smad3 signaling critically regulates fibroblast phenotype and function in healing myocardial infarction, Circ. Res. 107 (3) (2010) 418–428.
[32] P. Kong, A.V. Shinde, Y. Su, I. Russo, B. Chen, A. Saxena, et al., Opposing actions of fibroblast and cardiomyocyte Smad3 signaling in the infarcted myocardium, Circulation 137 (7) (2018) 707–724.
[33] B. Zhou, R. Tian, Mitochondrial dysfunction in pathophysiology of heart failure, J. Clin. Invest. 128 (9) (2018) 3716–3726.
[34] M. Liu, J. Lv, Z. Pan, D. Wang, L. Zhao, X. Guo, Mitochondrial dysfunction in heart failure and its therapeutic implications, Front Cardiovasc Med 9 (2022), 945142.
[35] A.A. Gibb, M.P. Lazaropoulos, J.W. Elrod, Myofibroblasts and fibrosis: mitochondrial and metabolic control of cellular differentiation, Circ. Res. 127 (3) (2020) 427–447.
[36] K. Mangkhang, V. Punyapornwithaya, P. Tankaew, W. Pongkan, N. Chattipakorn, C. Boonyapakorn, Plasma humanin as a prognostic biomarker for canine myxomatous mitral valve disease: a comparison with plasma NT-roBNP, Pol. J. Vet. Sci. 21 (4) (2018) 673–680.
[37] R.J. Widmer, A.J. Flammer, J. Herrmann, M. Rodriguez-Porcel, J. Wan, P. Cohen, et al., Circulating humanin levels are associated with preserved coronary endothelial function, Am. J. Physiol. Heart Circ. Physiol. 304 (3) (2013) H393–H397.
[38] S. Thummasorn, K. Shinlapawittayatorn, J. Khamseekaew, T. Jaiwongkam, S.C. Chattipakorn, N. Chattipakorn, Humanin directly protects cardiac mitochondria against dysfunction initiated by oxidative stress by decreasing complex I activity, Mitochondrion 38 (2018) 31–40.
[39] S. Thummasorn, N. Apaijai, S. Kerdphoo, K. Shinlapawittayatorn, S.C. Chattipakorn, N. Chattipakorn, Humanin exerts cardioprotection against cardiac ischemia/reperfusion injury through attenuation of mitochondrial dysfunction, Cardiovasc Ther 34 (6) (2016) 404–414.
[40] S. Thummasorn, K. Shinlapawittayatorn, S.C. Chattipakorn, N. Chattipakorn, High-dose Humanin analogue applied during ischemia exerts cardioprotection against ischemia/reperfusion injury by reducing mitochondrial dysfunction, Cardiovasc Ther 35 (5) (2017).
[41] L.E. Klein, L. Cui, Z. Gong, K. Su, R. Muzumdar, A humanin analog decreases oxidative stress and preserves mitochondrial integrity in cardiac myoblasts, Biochem. Biophys. Res. Commun. 440 (2) (2013) 197–203.
[42] H. Jin, T. Liu, W.-X. Wang, J.-H. Xu, P.-B. Yang, H.-X. Lu, et al., Protective effects of [Gly14]-Humanin on beta-amyloid-induced PC12 cell death by preventing mitochondrial dysfunction, Neurochem. Int. 56 (3) (2010) 417–423.
[43] S. Kumfu, S.T. Charununtakorn, T. Jaiwongkam, N. Chattipakorn, S.C. Chattipakorn, Humanin exerts neuroprotection during cardiac ischemia-reperfusion injury, J Alzheimers Dis 61 (4) (2018) 1343–1353.
[44] B. Guo, D. Zhai, E. Cabezas, K. Welsh, S. Nouraini, A.C. Satterthwait, et al., Humanin peptide suppresses apoptosis by interfering with Bax activation, Nature 423 (6938) (2003) 456–461.
[45] C. Lee, K. Yen, P. Cohen, Humanin: a harbinger of mitochondrial-derived peptides? Trends Endocrinol Metab 24 (5) (2013) 222–228.
[46] J. Burtscher, A. Soltany, N.P. Visavadiya, M. Burtscher, G.P. Millet, K. Khoramipour, et al., Mitochondrial stress and mitokines in aging, Aging Cell 22 (2) (2023), e13770.